Manuscript refereed by Dr José Garcia (Sandvik Machining Solutions, Sweden)

Influence of Heat Treatment and Densification on the Load Capacity of Sintered Gears

Scholzen, Philipp[1] *p.scholzen@wzl.rwth-aachen.de*; Rajaei, Ali[2] *a.rajaei@iwm.rwth-aachen.de*; Brimmers, Jens[1] *j.brimmers@wzl.rwth-aachen.de*; Hallstedt, Bengt[2] *b.hallstedt@iwm.rwth-aachen.de*; Bergs, Thomas[1,3] *t.bergs@wzl.rwth-aachen.de*; Broeckmann, Christoph[2] *c.broeckmann@iwm.rwth-aachen.de*

[1] Laboratory for Machine Tools and Production Engineering (WZL) of RWTH Aachen University, Campus-Boulevard 30, 52074 Aachen, Germany
[2] Chair and Institute for Materials Applications in Mechanical Engineering (IWM) of RWTH Aachen University, Augustinerbach 4, 52062 Aachen, Germany
[3] Fraunhofer Institute for Production Technology IPT, Steinbachstraße 17, 52074 Aachen

Abstract
The powder metallurgical manufacturing of gears offers a promising opportunity in terms of reducing the noise emission and increasing the power density. Sintered gears weigh less than conventional gears and potentially have a better noise-vibration-harshness behavior, due to the remaining porosity. However, the potential of sintered gears for highly loaded applications is not fully utilized yet. Six variants of surface densified and case-hardened sintered gears from Astaloy Mo85 are tested to analyze the impact of the densification and case hardening depths on both the tooth root and flank load bearing capacities. Experimental investigations including metallography and computer tomography are carried out to characterize the microstructure. Furthermore, a simulation model is developed to quantitatively describe the residual stress and hardness profiles after the heat treatment. The load bearing capacity was improved by increasing the densification and case hardening depths, where the effect of the case hardening was identified to be predominant.

Introduction and Motivation

As a result of climate change and the ambition to achieve optimum component properties, alternative process chains are increasingly becoming the focus of industry. In the context of electromobility, powertrains in particular are undergoing a current transformation. Gear transmissions are often used for power transmission and conversion. Powder metallurgical (PM) gears offer a potential alternative with regard to NVH-tailored design [1–5]. Due to the process-related porosity, components manufactured by powder metallurgy weigh up to 10% less than components made of cast metallurgical steel. Studies show a reduction in material usage due to the near-net-shape manufacturing of approx. 50% in the entire manufacturing chain of PM gears. In addition, PM gear manufacturing is attributed with up to 10% lower energy consumption compared to machining [6]. KLOCKE ET AL. quantify the economic advantages and quote a cost saving of 21.7% for the powder metallurgical process chain [7]. The powder metallurgical process chain for the manufacture of power gears includes powder production and mixing, pressing, the sintering process, and the cold rolling process [8]. This is followed by the conventional steps of gear manufacturing: Case hardening and grinding. After pressing and sintering, a component porosity of approx. 8-15% remains [9]. The remaining pores in the component lead to a reduced strength compared with melted steel gears, since the elastic modulus jump (from material to air) results in stress peaks under the influence of a stress field. Critical stresses on gears are mainly present in the surface zone of the tooth flank or tooth root, so that the surface zone is densified by the cold rolling process. This increases the load capacity of the gear [8]. After cold rolling, heat treatment is carried out by case hardening. Conventional process conditions with porosity can lead to undesirable case hardening depths and carbide precipitation [10, 11]. Therefore, the local density must be considered during heat treatment. However, for PM gears, there is currently a lack of reliable knowledge on the optimum choice of heat treatment parameters in combination with the local density profile.

Objective and Approach

The objective is the fundamental investigation of the influence of the case hardening and densification depths on the load bearing capacity of PM gears, based on simulation and experiment. To investigate the tooth root and tooth flank load bearing capacity, gear testing experiments are carried out and the material stress is simulated with regard to the local density. A total of six different variants with different combinations of densification and case hardening depths are investigated. All variants are first tested at fatigue strength levels for screening. For the reference variant and the variant with the highest potential, additional WÖHLER diagrams are determined. In parallel, a numerical simulation of the case hardening is carried out to quantitatively describe the evolution of the microstructure, hardness and the residual stress state. The required thermo-physical and mechanical material

© European Powder Metallurgy Association (EPMA)

properties depend on density, temperature, carbon content and microstructure. Most of the material data was adopted from [12]. However, further dilatometric investigations and metallographic characterizations are conducted for a better description of the transformation kinetics during quenching and tempering and the elastoplastic material behavior. Finally, the characterization of the test gears is used to validate the simulation. The model is evaluated regarding the predicted hardness and residual stress profiles for both heat treatment variants.

Method – Simulation method for heat treatment

The macro scale model applied in the present work is based on the early suggestions of INOUE [13] for a coupled modelling approach that comprises the calculation of heat transfer, phase transformations, transformation strains and the elastoplastic material response. The numeric modeling of the case hardening in this work is implemented in the commercial software ABAQUS FEA and considers the low-pressure carburizing (lpc), high pressure gas quenching (HPGQ) and tempering. The lpc-process is carried out by repeated cycles of boost and diffusion [14]. Accordingly, the process is modelled by setting the carbon content of the surface equal to the solubility of austenite during the boost time. During the diffusion stage, the carbon flux to the surface is equal to zero. To model the quenching and tempering stages, a coupled thermomechanical analysis is carried out. The main constitutive law in the mechanical analysis describes the evolution of the strains and assumes that the total strain rate is the sum of independent elastic, plastic, thermal and transformation induced strain rates. To describe the overall kinetics of the phase transformations, modified formulations and extensions of the KOISTINEN-MARBURGER equation [15] and the JOHNSON-MEHL-AVRAMI (JMA) equation [16] are suggested for the martensitic and the diffusion controlled transformations, respectively. More details about the modelling approach can be found in [12, 17]. Depending on the predicted microstructure and carbon content, the local hardness is calculated by an empirical model according to the quenching / tempering tests and hardness measurements. The hardness of bainite and martensite depend strongly on the carbon content. The model also covers the effect of the transformation temperature of bainite on the evolution of hardness. The model geometry and the mesh remain identical for all steps. To reduce the computational effort, the gear model is simplified by defining symmetry levels in a cylindrical coordinate system. The thermal boundary conditions (BC) describing the quenching stage are defined as the local heat transfer coefficient on the basis of the investigations for similar geometries and conditions under HPGQ [18]. In order to consider the effect of the densification depth, density profiles are determined by image analysis of the micrographs from the gears cross section. The distribution of the density is mapped to the model cross section as an initial condition of the numerical simulation.

Method – Conception of the investigation

The tooth root and tooth flank load bearing capacity are first determined separately in screening tests. The material and geometry data are shown in **Figure 1** on the left. The tooth root load bearing capacity and the tooth flank load bearing capacity are determined for six variants. Variation parameters are the case hardening depth CHD (C) and the densification depth (D). The case hardening depth CHD is varied in two steps, the densification depth in three steps. The densification and case hardening depths of the reference gear set were defined on the basis of the current industrial setting. For the reference, the case hardening depth is CHD_{Ref} = 0.1 - 0.2 m_n and the densification depth $t_{d,99}$ > 0.2 m_n (variant DH-CM). From the screening tests, the combination with the highest potential is selected to investigate the overall fatigue strength and for both the tooth root and the tooth flank load bearing capacity. The tests are carried out according to the FVA guideline [19].

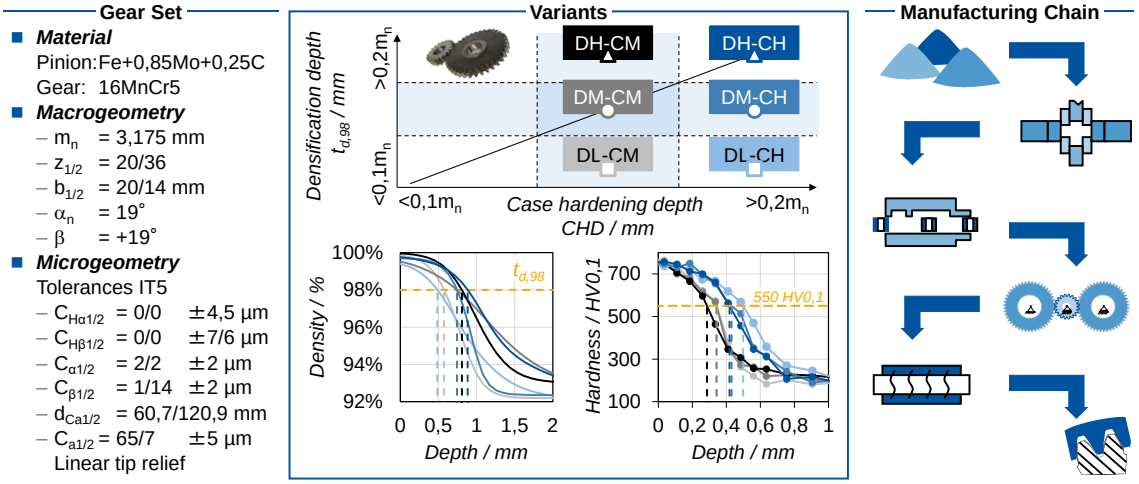


Figure 1: Variants and Characterization

© European Powder Metallurgy Association (EPMA)

The tooth flank load bearing capacity is determined in the back-to-back test rig (cf. [8]) by the endurance limit at one load level with a minimum of three tests per variant. The number of load cycles for a failure probability P_A = 50 % is determined using the WEIBULL evaluation method in the WEIBULL and GAßNER probability distribution. A load cycle number of $N = 5 \cdot 10^7$ load cycles is defined as the limit for the fatigue strength in accordance with the transition according to [20]. A total damage of all active tooth flanks of V_{Total} = 1 % or of a single tooth of V_{Tooth} = 4 % is evaluated as damage criterion [19]. The fatigue strength is investigated using the stair-step method with evaluation according to HÜCK [21].
The tooth root load capacity is investigated with the pulsator test rig (cf. [8]) by the endurance limit at one load level. Using the horizon method, the endurance limit is determined by five tests per variant. The number of load cycles for a failure probability P_A = 50 % is determined using the evaluation method according to ROSSOW with the WEIBULL probability distribution. The evaluation of the tolerable force amplitude (fatigue strength level) is performed using the stair-step method with evaluation according to HÜCK, where the limiting load cycle number is $N = 3 \cdot 10^6$ [21]. The damage criterion for determining the tooth root bearing capacity is tooth root fracture or breakage.

Results – Residual stresses and hardness

The actual process parameters of carburizing were confidential information of the project partner and therefore not shared. Thus, carburizing parameters had to be obtained for the simulation iteratively on the basis of measured carbon profiles on the tooth flank for both case hardening variants. The carbon profiles are determined by means of electron probe microanalysis. According to the simulation, the following carburizing parameters (boost time / diffusion time in minutes) are suggested for a carburizing temperature of 940°C:

- DH-CM: 2/9, 1.5/11, 1.5/15, 1.5/15 and 1/10
- DH-CH: 2.5/9, 2.5/11, 2/15, 2/20, 2/25 and 1/15

Hardness measurements and therefore the empirical modelling correspond to the micro hardness measure HV0.1, in order to obtain a porosity independent material property. **Figure 2** illustrates the comparison of the calculated carbon profiles and predicted hardness with corresponding experimental findings. The measured carbon content at the surface varies between 0.8 ma% and 0.85 ma% for both variants. The scatter of the measured values increases from the densification depth of the variants of 0.8 mm. The predicted surface hardness (≈780 HV0.1) lies slightly above the experimentally determined mean surface hardness of ≈750 HV0.1. The simulation predicts a CHD of approximately 0.445 mm and 0.57 mm for DH-CM and DH-CH, respectively, which is in a very good agreement with the measured hardness profiles (before grinding). The model predicted a martensitic surface zone with 6% retained austenite after tempering and a purely bainitic core, which agrees qualitatively with the experimental findings (not shown in the paper).

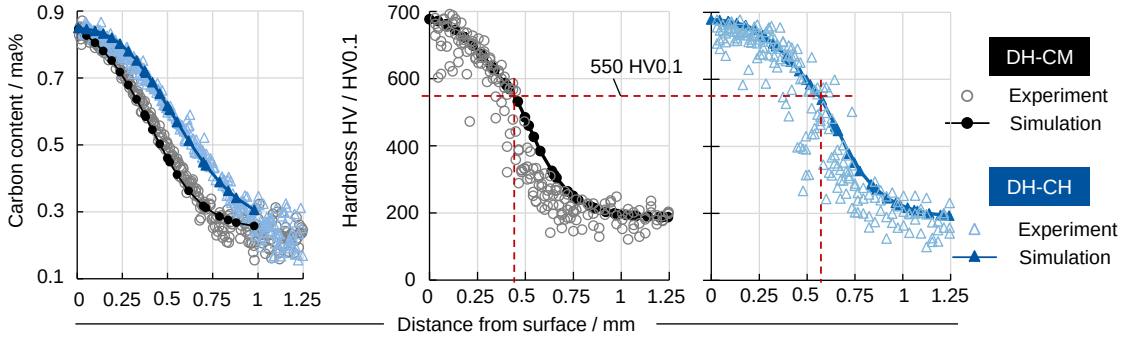


Figure 2: simulated and experimentally determined carbon content and hardness profiles

Figure 3 shows the tangential residual stress profiles in the tooth root and the tooth flank. Simulation results show a very good quantitative agreement with the measured stresses. Both simulation and experiment indicate compressive residual stresses in the surface zone, which is due to the transformation induced strains by the martensitic transformation. It can be seen that very high compressive stresses are induced in the flank surface due to the grinding process. This effect is not modelled in this work. The depth of the compressive stresses increases with the CHD. Surface stresses are not affected by the CHD in tooth root, but in the flank surface; a slight decrease of the compressive residual stresses is caused by increasing the CHD. This indicates that the load bearing capacity of the tooth flank is more likely to be affected by the CHD than that of the tooth root. Due to the fact, that the maximum stress under rolling contact is given under the flank surface, the increasing of the CHD could improve the load bearing capacity through the superposition of higher compressive residual stresses with the process loads in the subsurface volume.

© European Powder Metallurgy Association (EPMA)

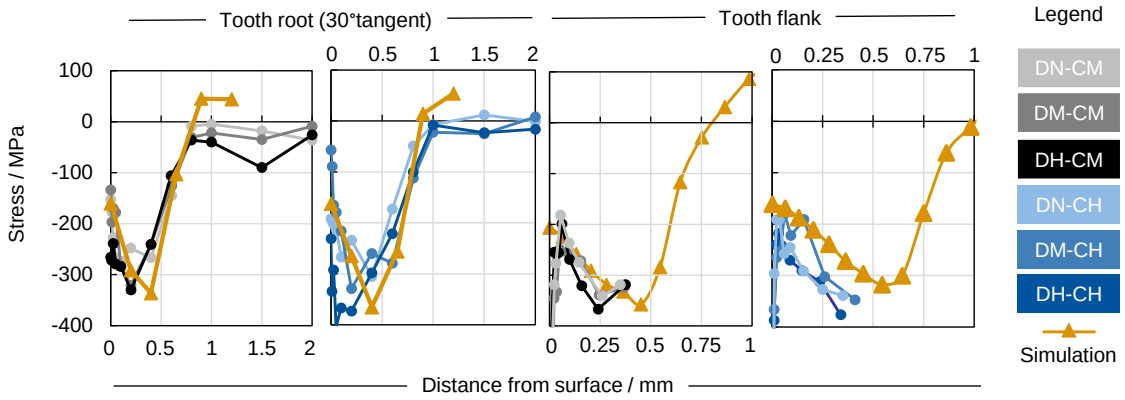


Figure 3: simulated and experimentally determined residual stress profiles

Results – Load capacity

The results of the investigations show that a high case hardening depth CHD ≈ 0.15m_n, compared to a medium case hardening depth CHD ≈ 0.1m_n, has a positive effect on the tooth root and tooth flank load bearing capacity of the test gears. As a result of the higher case hardening depth, a 6.5% increase in the fatigue strength level of the tooth root load bearing capacity is achieved. For the tooth flank load bearing capacity, on the other hand, an anti-proportional behavior of the load bearing capacity in relation to the densification depth is found for the average case hardening depth during the running tests in the back-to-back test rig (cf. **Figure 4**, Load cycles). The reason for this influence was identified as load-induced densification during operation of the tooth flanks, which can be measure by the negative profile- and lead-crowning c_α, c_β.

For the lower case hardening depth, a lower the densification depth of the variant leads to higher the load-induced densification. The densification results in a stress reduction in terms of lower contact pressures (cf. $\sigma_{H,max}$). An increase in the case hardening depth, on the other hand, causes a lower load-induced densification and an increase in the tooth flank load capacity independent of the densification depth.

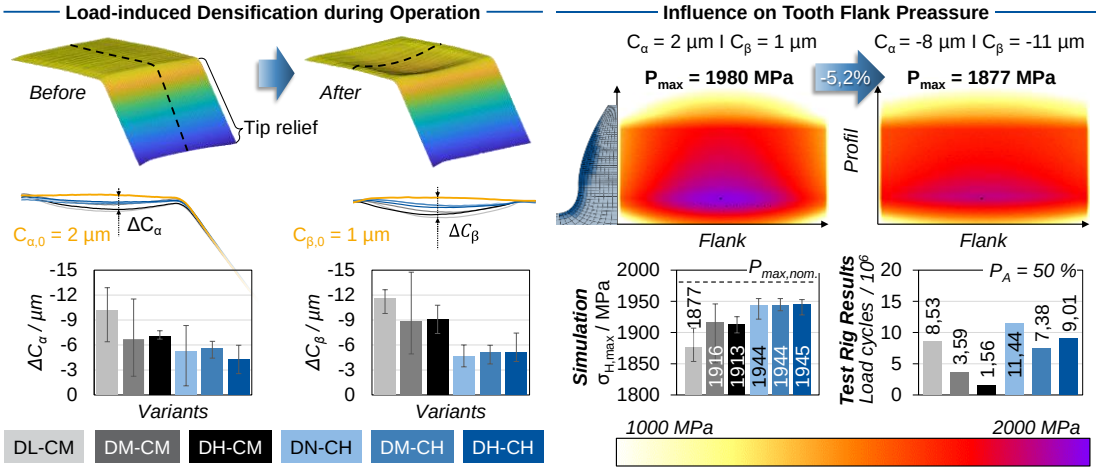


Figure 4: Load-induced densification during operation

Computed tomographic (CT) examinations of the teeth have identified the tooth flank surface as the location of damage initiation. Starting from smaller pittings there, crack propagation occurs at medium case hardening depth with a main crack growing behind the full densification zone towards the tooth tip, cf. **Figure 5**. For the crack propagation the crack propagates at a depth where a densification of ρ = 96% is present and where the microstructure is not hardened. In addition to the main crack, a fine crack network appears between the main crack and the surface.

For the variants with high case hardening depths, no main crack was identified on the pitch circle in the CT scan. The effect can be attributed to the stress-reducing compressive residual stresses due to the higher case depth. As a result of the residual stresses, a lower stress plateau is present at the critical local density of ρ = 96% for the variants with high case depth. As a result, the critical stress for crack growth is not reached. After the screening test, the DH-CH variant showed the highest potential regarding an increased load bearing capacity. Therefore, **Figure 6** shows the comparison of the fatigue behavior of the reference variant and the DH-CH variant.

© European Powder Metallurgy Association (EPMA)

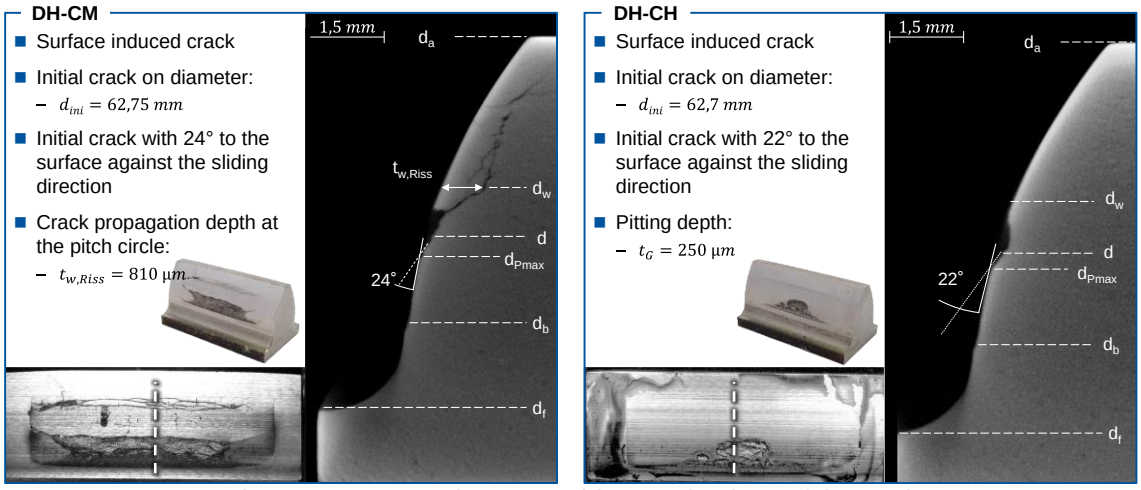


Figure 5: Computed tomographic examinations of the teeth

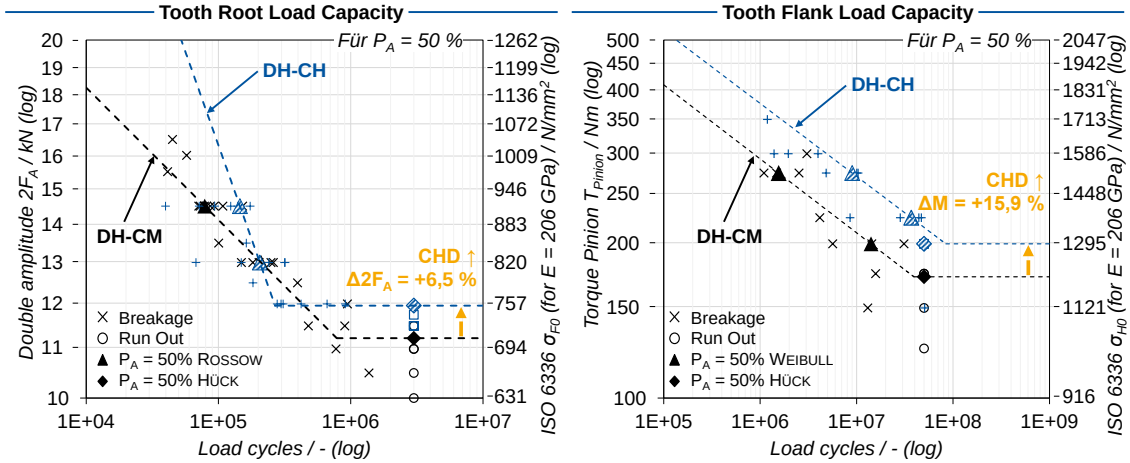


Figure 6: Fatigue behavior of the variants DM-CH and DH-CH

Overall, the results of the investigation show that the heat treatment and the densification process of powder metallurgy gears have a significant influence on the load capacity. In contrast to conventional melt-metallurgical gears, it is recommended to increase the case hardening depth of PM gears. The resulting higher residual compressive stresses counteract the lower stress resistance due to local porosity.

Summary and Outlook

Test rig trials were carried out on PM-gears, where six different variants with different combinations of densification and case hardening depths were investigated with regard to the resulting tooth root and tooth flank load bearing capacity. The test rig investigations have shown that a high case-hardening depth has a positive effect on the tooth root and tooth flank load bearing capacity of the test gears. In addition to the increase of the case-hardening depth, the increase of the densification depth also causes an increase of the tooth root load bearing capacity. In contrast, the running tests on the back-to-back test rig showed an anti-proportional behavior of the tooth flank load bearing capacity with respect to the densification depth for the medium case hardening depth. The reason for this influence was identified to be the densification of the tooth flanks during operation, which results in a stress reduction in the form of lower contact pressures. Using computer tomographic (CT) investigations of the teeth, the tooth flank surface could be identified as the location of crack initiation. Starting from the formed pitting on the surface, the crack propagates in variants with the medium case hardness depth into a distinct main crack, which grows behind the full densification zone towards the tooth tip. Besides the experimental investigation of the load capacity, a simulation model was developed for the quantitative description of the hardness and residual stress profiles after the heat treatment of the PM gears. The model is based on a continuum mechanical analysis of the thermomechanical and metallurgical processes arising in the material during the case hardening. Both simulation and experiment showed compressive residual stresses in the martensitic surface zone. An increase of the CHD leads to increasing the depth of the compressive stresses. The comparison between simulation

© European Powder Metallurgy Association (EPMA)

and experiment showed that the model describes the hardness and residual stresses in the carburized area very well.

Acknowledgement

The authors gratefully acknowledge the Federal Ministry for Economic Affairs and Energy for providing the financial support for the project [IGF 19025N] based on a resolution of the German Parliament and the support by the Research Association for Power Transmission Engineering (FVA)

References

[1] C. Brecher, C. Löpenhaus, and P. Scholzen, *Analysis of the Damping Potential of Powder Metallurgical Manufactured Gear Bodies: 14-18 October 2018, Bilbao Exhibition Centre (BEC), Bilbao, Spain*. Shrewsbury, United Kingdom: European Powder Metallurgy Association (EMPA), 2018.

[2] P. Scholzen, M. Andersson, C. Löpenhaus, and C. Brecher, *Improved NVH Behavior Of Transmission Gears By The Use Of PM: Euro PM2019 proceedings : 13-16 October 2018, Maastricht Exhibition & Congress Centre (MECC), Maastricht Netherlands*. Shrewsbury, United Kingdom: European Powder Metallurgy Association (EPMA), 2019.

[3] C. Brecher, C. Löpenhaus, M. Schroers, T. Frech, and P. Scholzen, “Optimization of NVH-Behavior of Gears by Alternative Gear Materials,” in *International Conference on Gears 2017*, Garching, 2017.

[4] G. Kotthoff, “NVH Potential of PM Gears for Electrified Drivetrains,” *Gear Technol. (Gear Technology)*, vol. 2018, no. 10, pp. 40–43, 2018.

[5] R. Hellein, A. Müller, and S. Zerobin, “Pulvermetallurgische Zahnradsysteme zur Optimierung von NVH-Eigenschaften in Verbrennungsmotoren,” in *Pulvermetallurgie in Wissenschaft und Praxis*, Band 35, *Pulvermetallurgie - Schlüsseltechnologie für innovative Systemlösungen: Vorträge und Ausstellerbeiträge des Hagener Symposiums am 28. und 29. November 2019 in Hagen*, H. Danninger, L. Sigl, and M. Schneider, Eds., Dortmund: Heimdall Verlag, 2019, 33-50.

[6] V. Kruzhanov and V. Arnhold, “Energy consumption in powder metallurgical manufacturing,” *Powder Metallurgy*, vol. 55, no. 1, pp. 14–21, 2012, doi: 10.1179/174329012X13318077875722.

[7] F. Klocke *et al., Eds., Hochfeste Zahnräder durch pulvermetallurgische Herstellungsverfahren*. Bonn, 2017.

[8] F. Klocke and C. Brecher, *Zahnrad- und Getriebetechnik: Auslegung - Herstellung - Untersuchung - Simulation,* 1st ed. München: Carl Hanser, 2017.

[9] P. Beiss, *Pulvermetallurgische Fertigungstechnik*. Berlin: Springer Vieweg, 2012.

[10] H. Altena and H. Danninger, “Wärmebehandlung von Sinterstahl-Präzisionsteilen: II. Prozess- und Anlagentechnik,” *BHM Berg- und Hüttenmännische Monatshefte*, vol. 150, no. 5, pp. 170–175, 2005.

[11] H. Danninger and M. Dlapka, “Heat Treatment of Sintered Steels–what is different?,” *HTM Journal of Heat Treatment and Materials*, vol. 73, no. 3, pp. 117–130, 2018.

[12] P. Nusskern, “Prozesssimulation der Herstellung einsatzgehärteter pulvermetallurgischer Bauteile,” Dissertation, Karlsruher Institut für Technologie, Karlsruhe, 2013.

[13] T. Inoue, T. Yamaguchi, and Z. Wang, “Stresses and phase transf. occurring in quenching of carburized steel gear wheel,” *Mater. Scien. and Tech.*, vol. 1, no. 10, pp. 872–876, 1985.

[14] V. Heuer, “Low-Pressure Carburizing,” *ASM Handbook, Steel Heat Treating Fundamentals and Processes*, Volume 4A, pp. 581–590, 2013.

[15] D. P. Koistinen and R. E. Marburger, “A general equation prescribing the extent of the austenite-martensite transformation in pure iron-carbon alloys and plain carbon steels,” *Acta Metallurgica*, vol. 7, no. 1, pp. 59–60, 1959.

[16] M. Avrami, “Granulation, phase change, and microstructure kinetics of phase change. III,” *The Journal of Chemical Physics*, vol. 9, no. 2, pp. 177–184, 1941.

[17] A. Eser, C. Broeckmann, and C. Simsir, “Multiscale modeling of tempering of AISI H13 hot-work tool steel – Part 2: Coupling predicted mechanical properties with FEM simulations,” *Computational Materials Science*, vol. 113, pp. 292–300, 2016.

[18] V. Heuer and K. Löser, “Experimentelles Verfahren zur Ermittlung von Wärmeübergangskoeff. bei der Hochdruck-Gasabschreckung,” *HTM Härtereitechnische Mitteilungen*, vol. 59, no. 6, pp. 432–438, 2004.

[19] *Empfehlungen zur Vereinheitlichung von Tragfähigkeitsversuchen an vergüteten und gehärteten Zylinderrädern*, FVA Nr. 563 I: Ausgabe 2012, FVA Forschungsvereinigung Antriebstechnik E.V., 2012.

[20] *Calculation of load capacity of spur and helical gears. Part 3: Calculation of tooth bending strength*, 6336-3, ISO INTERNATIONAL STANDARD, Berlin, 2019.

[21] M. Hück, “Ein verbessertes Verfahren für die Auswertung von Treppenstufenversuchen,” *Werkstofftechnik*, vol. 1983, no. 14, 406 bis 417, 1983.

© European Powder Metallurgy Association (EPMA)